Quasi-continuum models of twist-like and accordion-like low-frequency motions in DNA

Kuo-Chen Chou, Gerald M. Maggiora, and Boryeu Mao
Computational Chemistry, Upjohn Research Laboratories, Kalamazoo, Michigan 49001

ABSTRACT Formulae for calculating low-frequency twist-like and accordion-like modes of DNA molecules have been derived using a quasi-continuum model. The formulae can be employed in essentially all (viz. A, B, C, D, E, and Z) forms of DNA. Calculated results indicate that the experimentally observed low-frequency modes at 22 cm^{-1} for the A-form octanucleotide (d[CCCCGGGG]) and at 18 cm^{-1} for the B-form dodecanucleotide (d[CGCAA ATTTGCG]) may result from accordion-like motions, while those observed at 12 cm^{-1} and 15 cm^{-1} may result from combinations of twist-like oscillations excited in the intact segments of B- and A-DNA's, respectively. Frequency shifts in the low-frequency modes observed when DNA molecules undergo conformational changes among different forms are also discussed in terms of the current model.

I. INTRODUCTION

Recent spectroscopic work in a number of laboratories has provided evidence for the existence of low-frequency motions in proteins (Brown et al., 1972; Genzel et al., 1976; Painter et al., 1982) and DNA molecules (Painter et al., 1981; Urabe and Tominaga, 1982; Urabe et al., 1983; Lindsay et al., 1984; Wittlin et al., 1986; Lamba et al., 1989). Meanwhile, a number of models have been proposed and theoretical studies carried out to characterize these interesting internal motions (Suezaki and Gō, 1975; Chou and Chen, 1977; Levitt, 1978; Brooks and Karplus, 1982; Chou, 1983; Tidor et al., 1983; Chou, 1984; Levy et al., 1984; Ramstein and Lavery, 1988). An understanding of the nature of these motions, which generally involve the collective movement of many atoms, is an important prerequisite to understanding the molecular nature of macroscopic conformational changes and other related biochemical phenomena (Chou and Chen, 1977; Chou, 1988).

Recent work in our laboratory (Chou and Maggiora, 1988; Chou and Mao, 1988) based on a quasi-continuum model (Chou, 1986) has been concerned with exploring the nature and role of standing waves that may be excited within intact segments of DNA (Chou, 1984). These standing waves were shown to possess frequencies that, in general, lie in the region of the prominent 30 cm^{-1} Raman band observed by Painter et al. (1981). The narrow range of frequencies provides the possibility for resonance coupling amongst neighboring intact segments, which can lead to "quake-like" motions that may cause separation of the DNA strands sufficient to allow intercalation of very large drug molecules (Chou and Maggiora, 1988; Chou and Mao, 1988).

Raman bands lying below 30 cm^{-1} have also been observed in DNA molecules (Urabe and Tominaga, 1982; Urabe et al., 1983; Lindsay et al., 1984; Genzel et al., 1986; Lamba et al., 1989), indicating the existence of other types of low-frequency motions. The present work seeks to extend the quasi-continuum model used in our earlier work to the description of these motions, by considering twist- and accordion-like modes in DNA. As has been demonstrated in the previous work (Chou, 1986; Chou and Maggiora, 1988; Chou and Mao, 1988), quasi-continuum models provide a more macroscopic and thus global view of low-frequency, collective motions. Hence, an understanding of these motions may provide important insights into the molecular nature of many functions of biomacromolecular systems.

II. "RIBBONS-AND-SPRINGS" MODEL OF DOUBLE HELICAL DNA

For a biomacromolecule, the intramolecular interactions vary greatly in their strengths, as do the internal motions in their timescales. For example, the force-constant of a hydrogen bond is about two orders of magnitude smaller than that of a covalent bond, while the frequencies of fluctuating covalent bonds are two to three orders of magnitude greater than those of low-frequency collective motions (Chou and Chen, 1977). Thus it is possible, and sometimes desirable, to use different models to describe the high- and low-frequency internal motions of biomacromolecules.

When investigating high-frequency molecular motions

0006-3495/89/08/295/11 $2.00

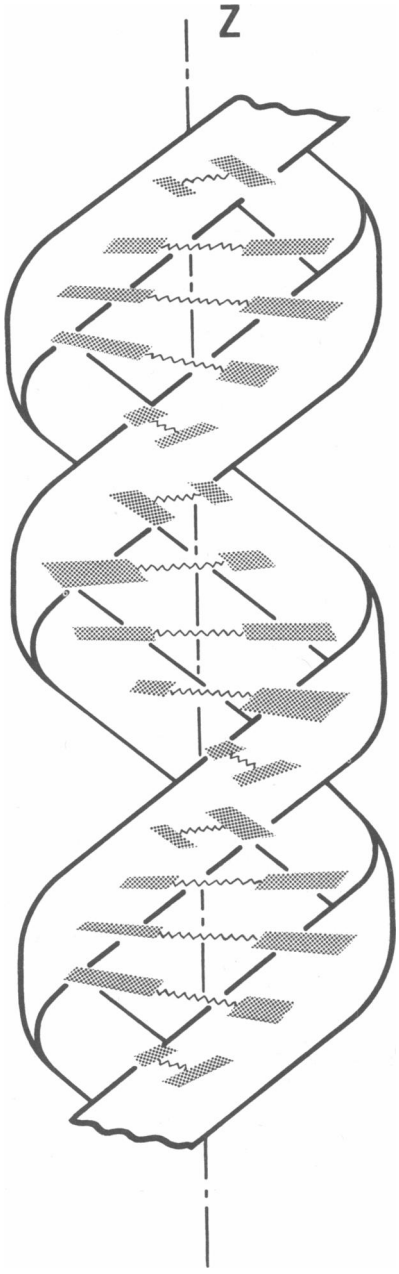

FIGURE 1 The "ribbons and springs" double twiner used to describe a DNA double helix structure from the viewpoint of quasi-continuum model. The two polynucleotide chains are compared with two helical ribbons intertwining around the Z-axis, and hydrogen bonds within a pair of complementary bases (denoted by hatched rectangles) are compared with a spring. The ribbons are held together by the springs which are related to one another by a rotation of an angle of θ_h around and a translation of z_h along the Z axis.

that arise from strong interactions between atoms and involve relatively small displacements, it is necessary to follow the detailed motions of individual atoms. Hence, it is necessary to use a discrete model. Low-frequency atomic motions, on the other hand, appear as collective motions of larger effective mass and include the motions of many atoms over larger distances. A detailed knowledge of the nature of high-frequency motions is relatively unimportant in low-frequency motions, because many fluctuations of a given atom about its average position will take place before a change in its average position occurs due to low-frequency collective motions (cf. Mao and McCammon, 1983). Therefore, low-frequency motions can be treated adiabatically and separated from the high-frequency fluctuations of individual atoms. Thus, discrete atomic models are unnecessary for describing low-frequency collective motions, and quasi-continuum models can provide a suitable means for treating such adiabatically separable systems. Moreover, quasi-continuum models afford a global and physically intuitive picture of low-frequency collective motions; and they provide a practical means for studying these motions in very large macromolecular systems.

In terms of the quasi-continuum model, the essential factors dominating low-frequency collective motions of biomacromolecules lie in the distribution of mass, in the arrangement of weak bonds, and in the overall system conformation. Within the quasi-continuum model a DNA double helix can be described by a "ribbons-and-springs" duplex (Chou, 1984; 1986) as shown in Fig. 1. In this model, the two polynucleotide chains are schematically depicted as helical ribbons intertwined about the Z axis, with the set of hydrogen bonds within a pair of complementary bases depicted as a mass-negligible spring which holds the double ribbons together. Each spring is related to its neighbors by a rotation θ_h about and a translation z_h along the Z axis. The sign and magnitude of these parameters depend on the type of DNA; e.g., for B-DNA $\theta_h = \pi/5$ and $z_h = 3.4$ Å, while for Z-DNA $\theta_h = -\pi/6$ and $z_h = 3.7$ Å. Positive values of θ_h correspond to right-handed helical ribbons and negative values correspond to left-handed helical ribbons. Through-space interactions between neighboring "springs" are neglected since contributions from such interactions need not be included as shown earlier (Chou, 1984). The classical work of Eysler and Prohofsky (1974) provides supportive evidence that through-space interactions between adjacent base pairs along a polynucleotide chain do not significantly influence the frequencies of low-frequency modes.

The double-helical ribbons can each also be viewed as ribbons which wrap around the surface of a virtual cylinder, as shown on Fig. 2. Thus, the curve which lies along the central line of each ribbon is given in Cartesian

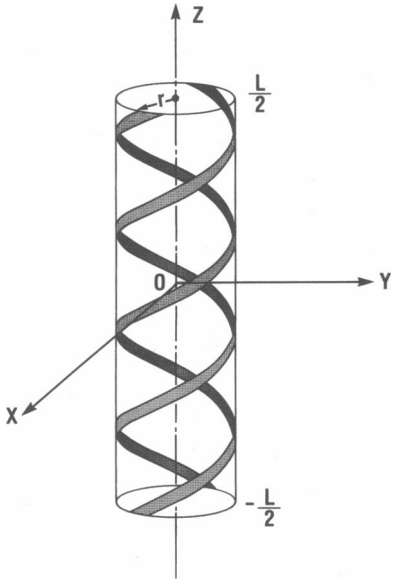

FIGURE 2 The DNA double-helical chain can also be compared with two ribbons wreathing around a virtual cylinder.

coordinates by the following equations

$$\begin{bmatrix} x_1 = r\cos(\theta z + \alpha_1) \\ y_1 = r\sin(\theta z + \alpha_1) \\ z_1 = z \end{bmatrix}, \quad \begin{bmatrix} x_2 = r\cos(\theta z + \alpha_2) \\ y_2 = r\sin(\theta z + \alpha_2) \\ z_2 = z \end{bmatrix}, \quad \left(-\frac{L}{2} \le z \le \frac{L}{2}\right) \tag{1}$$

or in cylindrical polar coordinates by the equations

$$\begin{bmatrix} r_1 = r \\ \phi_1 = \theta z + \alpha_1 \\ z_1 = z \end{bmatrix}, \quad \begin{bmatrix} r_2 = r \\ \phi_2 = \theta z + \alpha_2 \\ z_2 = z \end{bmatrix}, \quad \left(-\frac{L}{2} \le z \le \frac{L}{2}\right), \tag{2}$$

where r is the sum of the radius of the virtual cylinder and half of the thickness, if any, of the ribbon and

$$\theta = \frac{2\pi}{H}. \tag{3}$$

H being the pitch of the helical ribbon, i.e., the axial rise per turn. In Eq. 1 α_1 and α_2, the phase angles of ribbons 1 and 2, respectively, satisfy the following conditions:

$$|\alpha_2 - \alpha_1| = \xi = \begin{cases} 0.972\pi, & \text{for A-DNA} \\ 0.783\pi, & \text{for B-DNA} \\ 0.761\pi, & \text{for Z-DNA,} \end{cases} \tag{4}$$

which were derived from the work of Saenger (1984).

Define S as the absolute length of the ribbon, and L as the axial length measured by the Z-coordinates of the helical ribbon between its two ends. In the quasi-continuum model, the absolute length of the ribbon does not vary during an oscillation. Thus, it follows from Eqs. 1 or 2 that

$$\begin{aligned} S &= \int dS = \int \sqrt{(dx)^2 + (dy)^2 + (dz)^2} \\ &= \int_{-L/2}^{L/2} \sqrt{1 + r^2\theta^2}\, dz \\ &= \sqrt{1 + r^2\theta^2}\, L = \text{const.} \end{aligned} \tag{5}$$

The relationship among r, θ, and L depends on the type of oscillatory mode considered, and as will be shown in the following sections the internal displacement of the ribbon can generally be expressed in terms of the three components of a cylindrical polar coordinate system, viz.

$$\begin{bmatrix} u_r = u_r(z, t) \\ u_\phi = u_\phi(z, t) \\ u_z = u_z(z, t) \end{bmatrix}. \tag{6}$$

III. TWIST-LIKE OSCILLATIONS

When a DNA segment undergoes a twist-like oscillation as illustrated in Fig. 3 *a*,

$$u_z = 0 \tag{7}$$

and hence Eq. 6 reduces to

$$\begin{bmatrix} u_r = u_r(z, t) \\ u_\phi = u_\phi(z, t) \\ u_z = 0 \end{bmatrix}. \tag{8}$$

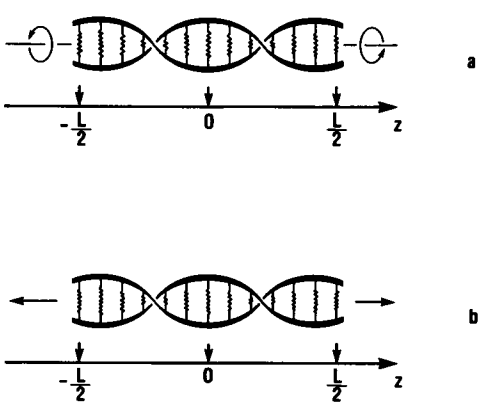

FIGURE 3 Illustration showing a DNA segment undergoing (*a*) the twist-like oscillation, and (*b*) the accordion-like oscillation.

In this case, the twist amplitude is greatest at the two ends and zero at the center of the double helix. If one assumes that the greatest twist angle (in radians) is λ, then displacement of the ϕ component along the DNA segment is given by

$$u_\phi(z,t) = \frac{2z\lambda}{L}\sin(\omega t) \quad \left(-\frac{L}{2} \le z \le \frac{L}{2}\right), \tag{9}$$

where ω is the angular frequency. On the other hand, from Eq. 7, we have

$$\Delta L = \int_{-L/2}^{L/2} d(\Delta z) = \int_{-L/2}^{L/2} du_z = \int_{-L/2}^{L/2} 0 dz = 0, \tag{10}$$

which shows that the axial length of the double helical ribbon, L, does not vary during torsional oscillations. Thus, according to Eq. 5, we have $r\theta$ = const., or

$$r\theta L = r\Phi = \text{const.}, \tag{11}$$

where

$$\Phi = \int_{-L/2}^{L/2} d\phi = \int_{-L/2}^{L/2} \theta dz = \theta L = \frac{2\pi}{H} L \tag{12}$$

is the total polar angle counted from one end of the ribbon to the other. Assuming that the variation in Φ due to a twist-like oscillation is $\Delta\Phi$, it follows from Eq. 11 that

$$\Delta r = -r\frac{\Delta\Phi}{\Phi}. \tag{13}$$

From Eq. 9 we have

$$\Delta\Phi(t) = \int_{-L/2}^{L/2} d(\Delta\phi) = \int_{-L/2}^{L/2} d\left(\frac{u_\phi}{r}\right) = 2\lambda \sin(\omega t) \tag{14}$$

so that

$$\Delta r(t) = u_r(z,t) = -\frac{2\lambda r}{\Phi}\sin(\omega t). \tag{15}$$

Substitution of Eqs. 9 and 15 into Eq. 8 yields

$$\begin{bmatrix} u_r = -\dfrac{2\lambda r}{\Phi}\sin(\omega t) \\ u_\phi = \dfrac{2z\lambda}{L}\sin(\omega t) \\ u_z = 0 \end{bmatrix}. \tag{16}$$

If ρ is the mass per unit length along the axis of the double helical ribbons, then the maximum kinetic energy of a mass element $\rho\Delta z$ of the double helical ribbons, at a distance z_i, is given by

$$\max(\Delta T_i) = \frac{\rho\Delta z}{2}\max\left(\frac{du}{dt}\right)_{z_i}^2 = \frac{\rho\Delta z}{2}\max[(r\dot{u}_\phi)^2 + \dot{u}_r^2]$$
$$= 2\rho r^2\lambda^2\omega^2\left(\frac{z_i^2}{L^2} + \frac{1}{\Phi^2}\right)\Delta z. \tag{17}$$

The total maximum kinetic energy of a DNA segment with axial length L is then given by

$$\max T = \lim_{\Delta z\to 0}\left[\sum_i \max(\Delta T_i)\right] = \int_{-L/2}^{L/2}\frac{2\rho r^2\omega^2\lambda^2}{L^2}\left(z^2 + \frac{L^2}{\Phi^2}\right)dz$$
$$= \frac{\rho r^2\omega^2 L\lambda^2}{6}\left[1 + \frac{12}{\Phi^2}\right]. \tag{18}$$

On the other hand, as shown in Fig. 4, a variation in r will change the length of the hydrogen bonds between complementary base pairs by

$$\Delta\ell(t) = 2\Delta r \sin\left(\frac{\xi}{2}\right) = -\frac{4\lambda r}{\Phi}\sin\left(\frac{\xi}{2}\right)\sin(\omega t). \tag{19}$$

Therefore, if the potential at the equilibrium position is assumed to be zero, the maximum potential due to such twist-like oscillations should be

$$\max U = \frac{nk_{base}[\max(\Delta\ell)]^2}{2} = \frac{8nk_{base}\sin^2(\xi/2)\, r^2\lambda^2}{\Phi^2}, \tag{20}$$

where k_{base} is the stretching force constant of the base pair, and n the number of base pairs. According to energy

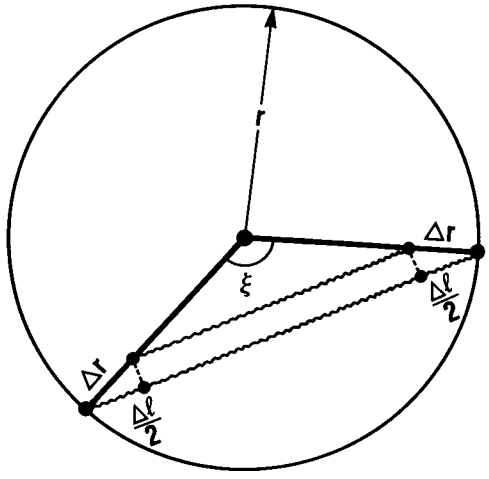

FIGURE 4 Illustration showing the variation $\Delta\ell$, of the length of a complementary hydrogen bond due to the variation of r, the sum of the radius of the virtual cylinder and half of the thickness of the ribbon (Fig. 2).

conservation, max T = max U, and thus it follows that

$$\omega^2 = \frac{48nk_{base}\sin^2(\xi/2)}{\rho L(\Phi^2+12)}. \tag{21}$$

Combining Eqs. 12 and 21 yields

$$\tilde{\nu} = \frac{\omega}{2\pi c} = \frac{2\sin(\xi/2)}{\pi c}\sqrt{\frac{3nk_{base}}{\rho L(\Phi^2+12)}}$$
$$= \frac{\sin(\xi/2)}{\pi^2 c}\sqrt{\frac{3k_{base}}{\langle m\rangle\left[1+(3/\pi^2)g^2(n)\right]}}\,g(n), \tag{22}$$

where ξ is given by Eq. 4, c is the speed of light in vacuum,

$$\langle m\rangle = \frac{\rho L}{n} = \frac{\text{total mass of the DNA molecule}}{\text{total number of its base pairs}} \tag{23}$$

and (Saenger, 1984)

$$g(n) = \frac{H}{L} = \begin{cases} \dfrac{11}{n}, & \text{for A-DNA} \\ \dfrac{10}{n}, & \text{for B-DNA} \\ \dfrac{9.33}{n}, & \text{for C-DNA} \\ \dfrac{8}{n}, & \text{for D-DNA} \\ \dfrac{7.5}{n}, & \text{for E-DNA} \\ \dfrac{12}{n}, & \text{for Z-DNA.} \end{cases} \tag{24}$$

IV. ACCORDION-LIKE OSCILLATIONS

Accordion-like oscillations in DNA segments depicted in Fig. 3*b*, represent another important class of low-frequency motions. In this case (cf. Eq. 7), we have

$$u_\phi = 0 \tag{25}$$

and hence Eq. 6 reduces to

$$\begin{bmatrix} u_r = u_r(z,t) \\ u_\phi = 0 \\ u_z = u_z(z,t) \end{bmatrix}. \tag{26}$$

Assuming that the maximum stretch at the two ends of the double helical ribbons is σ, the displacement of the ribbon in the z component due to the accordion-like oscillation is given by

$$u_z(z,t) = \frac{2z\sigma}{L}\sin(\omega t) \quad \left(-\frac{L}{2} \le z \le \frac{L}{2}\right). \tag{27}$$

When a helical ribbon undergoes accordion-like motion, however, it follows from Eq. 25 that

$$\Delta\Phi = \int_{-L/2}^{L/2} d(\Delta\phi) = \int_{-L/2}^{L/2} du_\phi = \int_{-L/2}^{L/2} 0dz = 0, \tag{28}$$

which means that Φ should remain invariant; i.e.,

$$\Phi = \theta L = \text{const.} \tag{29}$$

Thus, according to Eq. 5,

$$S^2 = L^2 + r^2\theta^2L^2 = L^2 + r^2\Phi^2 = \text{const.} \tag{30}$$

Assuming the variation in L due to accordion-like motion is ΔL, it follows from the above equation that

$$\Delta r = -\frac{L\Delta L}{r\Phi^2}. \tag{31}$$

Since from Eq. 27

$$\Delta L(t) = \int_{-L/2}^{L/2} d\Delta z = \int_{-L/2}^{L/2} du_z = 2\sigma\sin(\omega t) \tag{32}$$

it follows that

$$\Delta r(t) = u_r(z,t) = -\frac{2L\sigma}{r\Phi^2}\sin(\omega t). \tag{33}$$

Substitution of Eqs. 27 and 33 into Eq. 26 gives

$$\begin{bmatrix} u_r = -\dfrac{2L\sigma}{r\Phi^2}\sin(\omega t) \\ u_\phi = 0 \\ u_z = \dfrac{2z\sigma}{L}\sin(\omega t) \end{bmatrix}. \tag{34}$$

Following the same procedure used in deriving Eq. 18, the maximum kinetic energy of a DNA segment in accordion-like motion is given by

$$\max T = \lim_{\Delta z\to 0}\sum_i \frac{\rho\Delta z}{2}\max\left(\frac{du}{dt}\right)_{z_i}^2$$
$$= \int_{-L/2}^{L/2} 2\rho\omega^2\sigma^2\left(\frac{z^2}{L^2}+\frac{L^2}{r^2\Phi^4}\right)dz = \frac{\rho r^2\omega^2L\sigma^2}{6}\left(1+\frac{12L^2}{r^2\Phi^4}\right). \tag{35}$$

As a consequence of the variation in r, the lengths of the complementary hydrogen bonds will vary in a manner similar to that which occurs in twist-like motions. Thus,

variations in the length of the hydrogen bonds is given by (see Fig. 4 and cf. Eq. 19)

$$\Delta\ell(t) = 2\Delta r \sin\left(\frac{\xi}{2}\right) = \frac{-4L\sigma}{r\Phi^2} \sin\left(\frac{\xi}{2}\right) \sin(\omega t). \quad (36)$$

Therefore, the maximum potential due to such an accordion-like oscillation becomes

$$\max U = \frac{nk_{\text{base}}[\max(\Delta\ell)]^2}{2} = \frac{8nk_{\text{base}} \sin^2(\xi/2)\, L^2\sigma^2}{r^2\Phi^4}. \quad (37)$$

As energy conservation holds, it follows that max T = max U, and

$$\omega^2 = \frac{48nk_{\text{base}}L \sin^2(\xi/2)}{\rho r^2\Phi^4\left(1 + \frac{12L^2}{r^2\Phi^4}\right)}. \quad (38)$$

The corresponding wave number is then given by (cf. Eqs. 12 and 23)

$$\tilde{\nu} = \frac{\omega}{2\pi c} = \frac{2\sin(\xi/2)}{\pi c r\Phi^2}\sqrt{\frac{3nk_{\text{base}}L}{\rho\left(1 + \frac{12L^2}{r^2\Phi^4}\right)}}$$

$$= \frac{\sin(\xi/2)}{\pi^3 c}\left(\frac{H}{2r}\right)\sqrt{\frac{3k_{\text{base}}}{\langle m\rangle\left[1 + \frac{3}{\pi^4}\left(\frac{H}{2r}\right)^2 g^2(n)\right]}}\, g(n), \quad (39)$$

where $g(n)$ is given by Eq. 24, ξ by Eq. 4, and

$$\frac{H}{2r} = \begin{Bmatrix} 1.49, & \text{for A-DNA} \\ 2.06, & \text{for B-DNA} \\ 2.79, & \text{for Z-DNA} \end{Bmatrix}, \quad (40)$$

which were derived based on the following data (Saenger, 1984):

$$\begin{bmatrix} H = 28.2\ \text{Å}, & 2r = 18.9\ \text{Å}, & \text{for A-DNA} \\ H = 33.8\ \text{Å}, & 2r = 16.4\ \text{Å}, & \text{for B-DNA} \\ H = 44.4\ \text{Å}, & 2r = 15.9\ \text{Å}, & \text{for Z-DNA} \end{bmatrix}. \quad (41)$$

V. FORCE CONSTANT EVALUATION

The required force ("spring") constants, k_{base}, are computed based on the well-known feature of purine and pyrimidine base pairs in DNA that adenine (A) is bound to thymine (T) by two hydrogen bonds, and guanine (G) to cytosine (C) by three hydrogen bonds, as expressed schematically by A:::T and G:::C, respectively. Owing to these constraints, a homo-DNA double-helix structure must be either poly (A:::T) or poly (G:::C). Therefore, we have:

$$k_{\text{base}} = \begin{cases} 2k_h^s = 0.26 \times 10^5\ \text{dyn/cm} & \text{for poly (A:::T) DNA} \\ 3k_h^s = 0.39 \times 10^5\ \text{dyn/cm} & \text{for poly (G:::C) DNA,} \end{cases} \quad (42)$$

where k_h^s is the stretching force constant of a hydrogen bond (Itoh and Shimanouchi, 1970), and

$$\langle m\rangle = \begin{cases} 615\ g/N & \text{for poly (A:::T) DNA} \\ 616\ g/N & \text{for poly (G:::C) DNA,} \end{cases} \quad (43)$$

where N is the Avogadro constant. However, for a general DNA segment in which

$$\frac{[A] + [T]}{[G] + [C]} = \tau \quad (44)$$

we instead have

$$\left.\begin{aligned} k_{\text{base}} &= \left(\frac{2\tau + 3}{1 + \tau}\right) k_h^s \\ \langle m\rangle &= \left(\frac{615\tau + 616}{1 + \tau}\right) g/N \end{aligned}\right\}. \quad (45)$$

Specially, when $\tau = 1$, i.e., [A] + [T] = [G] + [C], we have

$$\begin{bmatrix} k_{\text{base}} = 2.5\, k_h^s = 0.325 \times 10^5\ \text{dyn/cm} \\ \langle m\rangle = 615.5\ \text{g}/N \end{bmatrix}. \quad (46)$$

Finally it is well to point out that although Eqs. 22 and 39, which describe low-frequency twist- and accordion-like modes, respectively, are derived based on isolated DNA segments containing n base pairs (cf. Fig. 3, *a* and *b*), they also can be used to calculate low-frequency motions of DNA segments that are part of much larger DNA duplexes if the segment is effectively isolated from the remainder of the molecule due to the rupture or deformation of hydrogen bonds at its two ends. Such deformations can arise from kinks in DNA, which persist for a time generally much longer than the periods typically observed for the low-frequency motions of interest in the current work (Levitt, 1978; Ramstein and Lavery, 1988). Intact segments in DNA molecules as defined in previous papers (Chou, 1984, 1986; Chou and Maggiora, 1988; Chou and Mao, 1988) are examples of such segments.

VI. RESULTS AND DISCUSSION

Tables 1 and 2 list the frequencies (in cm^{-1}) of twist-like and accordion-like oscillations calculated by Eqs. 24 and

TABLE 1 Wave numbers of twist-like motions calculated for A-, B-, and Z-DNA

	Wave number $\tilde{\nu}$ (cm^{-1})								
n*	A-DNA			B-DNA			Z-DNA		
	A:::T‡	G:::C§	Mix‖	A:::T‡	G:::C§	MIX‖	A:::T‡	G:::C§	MIX‖
6	38.0	46.5	42.6	34.2	41.8	38.1	36.9	45.2	41.2
8	32.3	39.5	33.9	28.6	35.0	32.0	31.8	38.9	35.4
10	27.7	33.9	31.0	24.4	29.8	27.2	27.5	33.6	30.7
12	24.1	29.5	27.1	21.1	25.8	23.5	24.0	29.4	26.9
15	20.1	24.5	22.4	17.4	21.3	19.5	20.1	24.6	22.5
18	17.1	20.9	19.1	14.8	18.1	16.5	17.2	21.0	19.2
24	13.1	16.0	14.7	11.3	13.8	12.6	13.2	16.2	14.8
38	8.4	10.3	9.4	7.3	8.9	8.1	8.5	10.5	9.6
50	6.5	7.9	7.2	5.6	6.8	6.2	6.6	8.1	7.3

*The number of base pairs in the DNA segment concerned.
‡Poly(A:::T) DNA segment.
§Poly(G:::C) DNA segment.
‖Poly(MIX) DNA segment with $\tau = \dfrac{[A] + [T]}{[G] + [C]} = 1$ (cf. Eqs. 44–45).

38, respectively, for various types and lengths of DNA segments. As will become evident in what follows, the data in the tables provide a basis for analyzing a number of features of the low-frequency motions of A-, B-, and Z-form DNAs.

First, examination of these tables shows that accordion-like oscillations have lower frequencies than twist-like oscillations generated in comparable DNA segments. For accordion-like oscillations, under similar conditions, the frequencies generated in A-DNA segments are lower than those in the B-DNA segments; while the frequencies generated in the B-DNA segments are lower than those in Z-DNA segments. For twist-like oscillations, however, the tendency is more complicated: under similar conditions, the frequencies generated in B-DNA segments are always lower than those in A- and Z-DNA segments, while the magnitudes of the frequencies between the A- and Z-DNA segments depend on n, the number of base pairs in a segment. In other words, if $\tilde{\nu}_A$, $\tilde{\nu}_B$, and $\tilde{\nu}_Z$ represent the low-frequency wave numbers excited in A-, B-, and Z-DNA segments, respectively, all the other conditions being similar, then

$$\left[\begin{array}{ll} \text{For twist-like oscillations:} & \begin{pmatrix} \tilde{\nu}_B < \tilde{\nu}_Z < \tilde{\nu}_A, & \text{when } n \le 12 \\ \tilde{\nu}_B < \tilde{\nu}_A \approx \tilde{\nu}_Z, & \text{when } n > 12 \end{pmatrix} \\ \text{For accordion-like oscillations:} & \tilde{\nu}_A < \tilde{\nu}_B < \tilde{\nu}_Z \end{array}\right]. \tag{47}$$

For DNA segments of the same type (e.g., A, B, or Z) and length (n), a poly (A:::T) DNA segment generates lower frequencies for both twist-like and accordion-like motions than the corresponding poly (G:::C) DNA segment. This follows because each base pair in poly (G:::C) DNA contains three hydrogen bonds, but each base pair in poly (A:::T) DNA contains only two hydrogen bonds. As the effective force constants of the base pairs, which hold the double helical ribbons (cf. Fig. 1), are relatively larger in G:::C rich DNA segments than in A:::T rich ones, it follows that poly (A:::T) DNA is more flexible than poly (G:::C) DNA, and hence the former will produce lower frequency twist-like and accordion-like oscillations.

Second, in a recent Raman study (Lamba et al., 1989) low-frequency peaks at 22 ± 2 cm^{-1} and 18 ± 2 cm^{-1} were observed in crystalline A-DNA [d(CCCCGGGG)] and B-DNA [d(CGCAAATTTGCG)] oligomers, respectively. According to the results presented in Table 2, the poly (G:::C) A-DNA segment with n = 8, which corresponds to the A-DNA [d(CCCCGGGG)] oligomers, possesses a low-frequency accordion-like oscillation with the wave number at 22.2 cm^{-1}, while the poly (Mix) B-DNA segment with n = 12 and τ = 1, which corresponds to the B-DNA [d(CGCAAATTTGCG)] oligomers, possesses a low-frequency accordion-like oscillation at 16.3 cm^{-1}. Both results are in excellent agreement with the experimental observations. However, for Z-DNA [d(CGCGCG)] oligomers, which according to the quasi-continuum model correspond to poly (G:::C) Z-DNA segments with n = 6, the calculated low-frequency accordion-like mode occurs at 42.6 cm^{-1}, while the corresponding observed value is 30 cm^{-1} (Lamba, et al., 1989). The inconsistency may be due to the inaccuracies in either the theoretical model or in the experimental observation. If the error comes from the theoretical model, it may be due either to the fact that it is more difficult to determine the parameters ξ and r accurately for Z-DNA making the result less reliable, or to the fact that a DNA segment with only six base pairs may be too short to be treated by the quasi-continuum ribbons-and-springs model.

Third, according to the report by Lindsay et al. (1984) low-frequency Raman bands at 12 cm^{-1} for B-DNA and 15 cm^{-1} for A-DNA have been observed. Such observations can be elucidated in terms of the quasi-continuum

TABLE 2 The wave numbers of accordion-like motions calculated for A-, B-, and Z-DNA

	Wave number $\tilde{\nu}$ (cm^{-1})								
n*	A-DNA			B-DNA			Z-DNA		
	A:::T‡	G:::C§	Mix‖	A:::T‡	G:::C§	MIX‖	A:::T‡	G:::C§	MIX‖
6	23.1	28.3	25.9	26.1	31.9	29.1	34.9	42.7	39.0
8	18.1	22.2	20.3	20.8	25.4	23.2	29.5	36.1	33.0
10	14.8	18.1	16.6	17.2	21.0	19.2	25.3	30.9	28.2
12	12.5	15.3	14.0	14.6	17.8	16.3	21.9	26.8	24.5
15	10.1	12.3	11.3	11.8	14.5	13.2	18.2	22.3	20.3
18	8.5	10.3	9.5	9.9	12.2	11.1	15.5	18.9	17.3
24	6.4	7.8	7.1	7.5	9.2	8.4	11.8	14.5	13.3
38	4.0	5.0	4.5	4.8	5.9	5.3	7.6	9.3	8.5
50	3.1	3.8	3.4	3.6	4.5	4.1	5.8	7.1	6.5

*,‡,§,‖See the corresponding footnotes to Table 1.

model as follows. As discussed earlier, the formulae derived here can also be employed to calculate the low-frequency motions of a DNA molecule if it is assumed that the DNA is made up of smaller intact segments. An intact segment is defined as a tract of double stranded DNA whose hydrogen bonds are intact, viz. not significantly distorted from their equilibrium states, and whose boundaries are formed by ruptures or substantial structural distortions in the complementary base pairs (Chou, 1984, 1986; Chou and Maggiora, 1988; Chou and Mao, 1988). Assuming that under the condition of the observations a typical intact segment has 24 base pairs (Mandel et al., 1979) and an equimolar mixture of A:::T and G:::C base pairs (i.e., $n = 24$ and $\tau = 1$, respectively), twist-like motions should, according to the quasi-continuum model, possess low-frequency oscillations of 12.6 cm^{-1} and 14.7 cm^{-1} for B- and A-form DNAs, respectively (see Table 1), both of which lie close to the corresponding observed values of 12 cm^{-1} and 15 cm^{-1} (Lindsay et al., 1984). Hence, the origin of the two observed low-frequency peaks may be due to twist-like oscillations of many such intact segments (Chou and Maggiora, 1988; Chou and Mao, 1988) in B-DNA and A-DNA, respectively.

According to the observations of Urabe and his coworkers (Urabe and Tominaga, 1982; Urabe et al., 1983), however, when DNA undergoes a conformational change from A to B form, the 22 cm^{-1} mode of the A-DNA changes to the 16 cm^{-1} mode of B-DNA. A comparison between Lindsay et al.'s results and Urabe et al.'s results indicates a common tendency: the magnitude of observed low-frequency value increases in going from B- to A-DNA. Such a tendency is fully reflected by the calculated results (cf. Table 1) for twist-like oscillations. The relatively higher values observed by Urabe et al. (1983) suggests that the intact segments may be relatively shorter (Table 1) than those investigated by Lindsey et al. (1984), i.e., there is more disorder in the double-helix under the experimental conditions used by Urabe, et al. (1983). This can be rationalized by the different experimental conditions under which the low-frequency modes were observed by Urabe et al. (1983) and by Lindsay et al. (1984). The average length of the intact segments will be changed in different conditions because it is determined by the equilibrium constant between open base pairs and closed base pairs (Chou, 1984). From the calculations and discussion the following two important features emerge that support twist-like rather than accordion-like oscillations as those responsible for the low-frequency motions observed by Urabe et al. (1983) and Lindsay et al. (1984): (*a*) the magnitude of calculated values for twist-like oscillations increases in going from B- to A-DNA as observed (Urabe et al., 1983; Lindsay et al., 1984), while the opposite is true for accordion-like oscillations, and (*b*) the size of the intact segments required for accordion-like oscillations with frequencies comparable with those observed (Urabe et al., 1983; Lindsay et al., 1984) would be much shorter than has been observed for such segments (Mandel, 1979).

A wide variety of experimental data (Horowitz and Wang, 1984; Miller, 1979; Hagerman, 1988; Hurley et al., 1980) have been interpreted by the elastic rod model of DNA. The torsional force constant, or torsional rigidity, deduced from those studies lies in the region of 10^{-19} erg-cm (Horowitz and Wang, 1984; Miller, 1979; Hagerman, 1988; Hurley et al., 1980). Using the torsional force constant, the maximum potential energy of a DNA segment due to twist-like oscillations can be expressed as (Barkley and Zimm, 1979)

$$\max U = \frac{k_T}{2}\left[\frac{\max (\Delta\Phi)^2}{L}\right] = \frac{2k_T\lambda^2}{L}, \tag{48}$$

where k_T is the torsional force constant. Note that here k_T corresponds to the symbol C generally adopted by other investigators (Horowitz and Wang, 1984; Miller, 1979; Hagerman, 1988; Hurley et al., 1980). From Eq. 18 employing a similar procedure to that used in deriving Eqs. 21 and 22 gives

$$\omega^2 = \frac{12k_T}{\rho r^2 L^2\left(1 + \frac{12}{\Phi^2}\right)} \tag{49}$$

and

$$\tilde{\nu} = \frac{\omega}{2\pi c} = \frac{1}{\pi c}\sqrt{\frac{3k_T g(n)}{n\langle m\rangle r^2 H\left[1 + \frac{3}{\pi^2}g^2(n)\right]}}. \tag{50}$$

Based on experimental data, Horowitz and Wang (1984) estimated a value of 3.0×10^{-19} erg-cm for k_T, which represents a lower limit. Miller (1979), using a purely theoretical approach, proposed a value of 20×10^{-19} erg-cm. However, substituting either value of k_T into Eq. 50 produces frequencies (in cm^{-1}) significantly below those observed experimentally. Even Miller's estimate, which is generally larger than most, leads to values about five times smaller than those observed experimentally for twist-like oscillations. A possible source for this discrepancy may be the fact that torsional force constant estimates are generally inferred from experiments that describe torsional motions indirectly. In addition, it is generally assumed that values derived in those studies represent lower limits to k_T (Hurley et al., 1980).

To derive k_T directly from torsional motion, it follows from Eqs. 20 and 48 that

$$k_T = \frac{ng(n)}{\pi^2} k_{base} H r^2 \sin^2\left(\frac{\xi}{2}\right), \tag{51}$$

which, upon substitution of Eq. 24, yields

$$k_T = \begin{cases} \frac{11}{\pi^2} k_{base} H r^2 \sin^2\left(\frac{\xi}{2}\right), & \text{for A-DNA} \\ \frac{10}{\pi^2} k_{base} H r^2 \sin^2\left(\frac{\xi}{2}\right), & \text{for B-DNA} \\ \frac{9.33}{\pi^2} k_{base} H r^2 \sin^2\left(\frac{\xi}{2}\right), & \text{for C-DNA} \\ \frac{8}{\pi^2} k_{base} H r^2 \sin^2\left(\frac{\xi}{2}\right), & \text{for D-DNA} \\ \frac{7.5}{\pi^2} k_{base} H r^2 \sin^2\left(\frac{\xi}{2}\right), & \text{for E-DNA} \\ \frac{12}{\pi^2} k_{base} H r^2 \sin^2\left(\frac{\xi}{2}\right), & \text{for Z-DNA} \end{cases} \quad (52)$$

where ξ, H, and r are given by Eqs. 4 and 41 and depend on the type of DNA. Thus, from Eq. 52 it is possible to calculate the torsional force constants for various types of DNA directly using a quasi-continuum approach as described above.

Stretching force constants can be obtained similarly. Assuming k_S is the stretching force constant of an intact DNA segment with unit length, then the maximum potential energy of such a segment due to accordion-like oscillation can be expressed as

$$\max U = \frac{k_S}{2}\left[\frac{\max (\Delta L)^2}{L}\right] = \frac{2k_S\sigma^2}{L}. \quad (53)$$

Combining the above equation with Eq. 37 yields

$$k_S = \frac{ng(n)}{4\pi^2 r^2} k_{base} H^3 \sin^2\left(\frac{\xi}{2}\right), \quad (54)$$

which upon substitution of Eq. 24 gives

$$k_S = \begin{cases} \frac{11}{4\pi^2 r^2} k_{base} H^3 \sin^2\left(\frac{\xi}{2}\right), & \text{for A-DNA} \\ \frac{5}{2\pi^2 r^2} k_{base} H^3 \sin^2\left(\frac{\xi}{2}\right), & \text{for B-DNA} \\ \frac{9.33}{4\pi^2 r^2} k_{base} H^3 \sin^2\left(\frac{\xi}{2}\right), & \text{for C-DNA} \\ \frac{2}{\pi^2 r^2} k_{base} H^3 \sin^2\left(\frac{\xi}{2}\right), & \text{for D-DNA} \\ \frac{7.5}{4\pi^2 r^2} k_{base} H^3 \sin^2\left(\frac{\xi}{2}\right), & \text{for E-DNA} \\ \frac{3}{\pi^2 r^2} k_{base} H^3 \sin^2\left(\frac{\xi}{2}\right), & \text{for Z-DNA,} \end{cases} \quad (55)$$

where ξ, H, and r are also dependent on the type of DNA (cf. Eqs. 4 and 41).

Table 3 lists the torsional and stretching force constants for A-, B-, and Z-DNA calculated from Eqs. 52 and 55, respectively, which shows that the torsional force constant, k_T, is about two orders of magnitude greater than the lower limits estimated in references 21 and 23. Also it can be seen that B-DNA has smaller values of the torsional force constant than either A- or Z-DNA. For the stretching force constant, however, Z-DNA has larger values than B-DNA, and B-DNA has larger values than A-DNA.

Overall, the quasi-continuum model provides a conceptually simple picture of the mechanical properties of DNA (and RNA) duplexes in the low-frequency regime. It should be pointed out, however, that the current model is a linear one, and thus nonlinear effects are not included, which is not to say that such effects are unimportant. In fact along with reductions in symmetry of the physical system (which can occur, e.g., by bending along the helix axis), nonlinear effects can serve to couple the twist-like and accordion-like modes described here. Nevertheless, as the frequencies of two types of modes for a given DNA duplex are not in resonance, we feel that coupling effects will not dominate but rather will tend to modulate the two oscillatory modes.

VII. SUMMARY AND CONCLUSIONS

In addition to low-frequency standing waves excited in the intact segments of DNA molecules, it is seen that twist- and accordion-like oscillations represent two other types of low-frequency modes that can be excited in DNA molecules as well. Accordion-like motions generated in DNA segments have lower frequencies than twist-like motions generated in equivalent segments. The experimental lowest-frequency modes observed for octanucleotide A-DNA [*d*(CCCCGGG G)] and dodecanucleotide B-DNA [*d*(CGCAAATTTGCG)] crystals (Lamba, 1989) are very likely due to accordion-like motions. The observed low-frequency modes of DNA molecules (Urabe and Tominaga, 1982, Urabe et al., 1983, Lindsay et al., 1984), however, might be due to the twist-like oscillations excited in their intact segments. Finally, both the torsional and stretching force constants for different types of DNA have been derived. The torsional force constants found here are about two orders of magnitude greater than the lower-limits as usually estimated indirectly from a variety of experiments such as fluorescence depolarization of bound ligands.

Thus, it appears that the quasi-continuum model can provide a reasonable description of several of the most important low-frequency modes undergone by double-helical DNAs. Moreover, the simple mechanical picture provided by the quasi-continuum model may be useful as

TABLE 3 The torsional and stretching force constants calculated for A-, B-, and Z-DNA

Type of force constant	A-DNA			B-DNA			Z-DNA		
	A:::T	G:::C	MIX	A:::T	G:::C	MIX	A:::T	G:::C	MIX
k_τ^* (10^{-17} erg-cm)	7.28	10.9	9.11	5.32	7.98	6.65	7.68	11.5	9.60
$k_S^\ddagger$ (10^{-2} dyn)	1.82	2.72	2.27	3.36	5.04	4.20	9.48	14.2	11.8

*Torsional force constant per unit length of DNA.
‡Stretching force constant per unit length of DNA.
See the footnotes of Table 1 for further explanation.

a basis for interpreting complex physico-chemical experiments designed to study the nature of the biologically relevant low-frequency motions of this important class of biomacromolecules.

Received for publication 30 November 1988 and in final form 7 April 1989.

REFERENCES

Barkley, M. D., and B. H. Zimm. 1979. Theory of twisting and bending of chain macromolecules; analysis of the fluorescence depolarization of DNA. *J. Chem. Phys.* 70:2991–3006.

Brooks, B., and M. Karplus. 1982. Harmonic dynamics of proteins: Normal modes and fluctuations in bovine pancreatic trypsin inhibitor. *Proc. Natl. Acad. Sci. USA.* 80:6571–6575.

Brown, K. G., S. C. Erfurth, E. W. Small, and W. L. Peticolas. 1972. Conformationally dependent low-frequency motions of proteins by laser Raman spectroscopy. *Proc. Natl. Acad. Sci. USA.* 69:1467–1469.

Chou, K. C. 1983. Identification of low-frequency modes in protein molecules. *Biochem. J.* 215:465–469.

Chou, K. C. 1984. Low-frequency vibrations of DNA molecules. *Biochem. J.* 221:27–31.

Chou, K. C. 1985. Low-frequency motions in protein molecules: β-sheet and β-barrel. *Biophys. J.* 48:289–297.

Chou, K. C. 1986. Origin of low-frequency motions in biological macromolecules: a view of recent progress in the quasi-continuum model. *Biophys. Chem.* 25:105–116.

Chou, K. C. 1988. Low-frequency collective motion in biomacromolecules and its biological functions. *Biophys. Chem.* 30:3–48.

Chou, K. C., and N. Y. Chen. 1977. The biological functions of low-frequency phonons. *Sci. Sin.* 20:447–457.

Chou, K. C., and G. M. Maggiora. 1988. Biological functions of low-frequency vibrations (phonons): 7. The impetus for DNA to accommodate intercalators. *Br. Polym. J.* 20:143–148.

Chou, K. C., and B. Mao. 1988. Collective motion in DNA and its role in drug intercalation. *Biopolymers.* 27:1795–1815.

Eyster, J. M., and E. W. Prohofsky. 1974. Lattice vibrational modes of poly (rU) · poly (rA): a coupled single-helical approach. *Biopolymers.* 13:2527–2543.

Genzel, L., F. Keilmann, T. P. Martin, G. Winterling, Y. Yacoby, H. Fröhlich, and M. W. Makinen. 1976. Low-frequency Raman spectra of lysozyme. *Biopolymers.* 15:219–225.

Hagerman, P. J. 1988. Flexibility of DNA. *Annu. Rev. Biophys. Biophys. Chem.* 17:265–286.

Horowitz, D. S., and J. C. Wang. 1984. Torsional rigidity of DNA and length dependence of the free energy of DNA supercoiling. *J. Mol. Biol.* 173:75–91.

Hurley, I., B. H. Robinson, C. P. Scholes, and L. S. Lerman. 1980. Torsional flexibility of DNA as determined by electron paramagnetic resonance. *in* Nucleic Acid Geometry and Dynamics. by R. H. Sarma, editor. Pergamon Press, New York. 253–271.

Itoh, K., and T. Shimanouchi. 1970. Vibrational frequencies and modes of α-helix. *Biopolymers.* 9:383–399.

Lamba, O. P., A. H. J. Wang, and G. J. Thomas Jr. 1989. Low-frequency dynamics and Raman scattering of crystals of B, A, and Z-DNA and fibers of C-DNA. *Biopolymers.* 28:667–678.

Levitt, M. 1978. How many base-pairs per turn does DNA have in solution and in chromatin? Some theoretical calculations. *Proc. Natl. Acad. Sci. USA.* 75:640–644.

Levy, R. M., A. R. Srinivasam, W. K. Olson, and J. A. McCammon. 1984. Quasi-harmonic method for studying very low frequency modes in proteins. *Biopolymers.* 23:1099–1112.

Lindsay, S. M., J. W. Powell and A. Rupperecht. 1984. Observation of low-lying Raman bands in DNA by tandem interferometry. *Phys. Rev. Lett.* 53:1853–1855.

Mandal, C., N. R. Kallenbach, and S. W. Englander. 1979. Base-pair opening and closing reactions in the double helix: A stopped-flow hydrogen exchange study in poly (rA) · poly (rU). *J. Mol. Biol.* 135:391–411.

Mao, B., and J. A. McCammon. 1983. Hinge-bending in L-arabinose binding protein: A theoretical study of the internal energy and free energy. *J. Biol. Chem.* 258:12543–12547.

Miller, K. J. 1979. Interactions of molecules with nucleic acids. I. An algorithm to generate nucleic acid structures with an application to the B-DNA structure and counterclockwise helix. *Biopolymers.* 18:959–980.

Painter, P. C., L. E. Mosher, and C. Rhoads. 1981. Low-frequency modes in the Raman spectrum of DNA. *Biopolymers.* 20:243–247.

Painter, P. C., L. E. Mosher, and C. Rhoads. 1982. Low-frequency modes in the Raman spectra of proteins. *Biopolymers.* 21:1469–1472.

Ramstein, J., and R. Lavery. 1988. Energetic coupling between DNA bending and base pair opening. *Proc. Natl. Acad. Sci. USA.* 85:7231–7235.

Saenger, W. 1984. Principles of Nucleic Acid Structure. Chap. 9. Springer-Verlag GmbH & Co. K. G., Heidelberg, Berlin.

Suezaki, Y., and N. Gō. 1975. Breathing mode of conformational fluctuations in globular proteins. *Int. J. Pept. Protein Res.* 7:333–334.

Tidor, B., K. K. Irikura, B. R. Brooks, and M. Karplus. 1983. Dynamics of DNA oligomers. *J. Biomol. Struct. & Dyn.* 1:231–252.

Urabe, H., and Y. Tominaga. 1982. Low-lying collective modes of DNA double helix by Raman spectroscopy. *Biopolymers.* 21:2477–2481.

Urabe, H., Y. Tominaga, and K. Kubota. 1983. Experimental evidence of collective vibrations in DNA double helix Raman spectroscopy. *J. Chem. Phys.* 78:5937–5939.

Wittlin, A., A. W. Genzel, F. Kremer, S. Häseler, A. Poglitsch, and A. Rupprecht. 1986. Far-infrared spectroscopy on oriented films of dry and hydrated DNA. *Phys. Rev. A.* 34:493–500.